Supplementary Information

A Steric Effect on the Nucleophilic Reactivity of Nickel(III)-Peroxo Complexes

Jalee Kim,[1,‡] Bongki Shin,[1,‡] Hyunjeong Kim,[1] Junhyung Lee,[1] Joongoo Kang,[1] Sachiko Yanagisawa,[2] Takashi Ogura,[2] Hideki Masuda,[3] Tomohiro Ozawa,[3] and Jaeheung Cho*[1]

[1]*Department of Emerging Materials Science, DGIST, Daegu 711-873, Korea*

[2]*Department of Frontier Materials, Graduate School of Engineering, Nagoya Institute of Technology, Gokiso, Showa, Nagoya 466-8555, Japan*

[3]*Picobiology Institute, Graduate School of Life Science, University of Hyogo, Koto 3-2-1, Kamigori-cho, Ako-gun, Hyogo 678-1297, Japan*

[‡]These authors contributed equally.

*To whom correspondence should be addressed.

E-mail: jaeheung@dgist.ac.kr

Experimental Section

Synthesis of Ligands

Pyridine-2,6-dicarbaldehyde (L1). We have modified the published method by using SeO_2 and 1,4-dioxane to obtain **L1**.[1] Yield: 5.12 g (71%), ^{1}H NMR ($CDCl_3$, 400 MHz): 8.07 (1H, t, PyH), 8.16 (2H, d, PyH), 10.15 (2H, s, CH).

***N,N'*-(pyridine-2,6-diylbis(methylene))dicyclohexylamine (L2).** To a stirred ethanol solution of **L1** (13 g, 10 mmol) was added cyclohexylamine (2.86 mL, 25 mmol) over 1 hour. Upon stirring for 6 hours, excess $NaBH_4$ was added to the mixture, which was further stirred for several hours. The solution was filtered and evaporated under reduced pressure. An ordinary work-up treatment of the reaction mixture with NaOH followed by extraction with $CHCl_3$ and evaporation gave an organic product. Yield: 2.38 g (88%), ^{1}H NMR ($CDCl_3$, 400 MHz): ~1.08 (12H, m, CH_2), ~1.70 (8H, m, CH_2), 2.40 (2H, s, CH), 3.82 (4H, s, CH_2), 7.05 (2H, d, PyH), 7.48 (1H, t, PyH).

2,6-bis(chloromethyl)pyridine (L3). To a stirred Et_2O solution of 2,6-bis(hydroxymethyl)pyridine (6.33 g) in an ice bath was slowly added thionyl chloride (7.29 mL). The mixture was then warmed on the water bath for 20 hours, during which time a white precipitate formed. The precipitate was collected by filteration. The solid was dissolved in water treated with $NaHCO_3$. The mixture was extracted with ethyl acetate. The solvent was removed under reduced pressure to yield **L3**, as a white solid. Yield: 8.82 g (91 %), ^{1}H NMR ($CDCl_3$, 400 MHz): 4.66 (4H, s, CH_2), 7.45 (2H, t, CH), 7.76 (1H, t, PyH).

***N,N'*-di-cyclohexyl-2,11-diaza[3,3](2,6)pyridinophane (CHDAP). L2** (0.498 g, 2 mmol) in DMF and sodium carbonate (0.15 g) were heated at reflux. A DMF solution of **L3** (0.603 g, 3.4 mmol) was then added dropwise to the mixture over 1 hour while stirring. After adding an ice water, a white powder precipitated and was filtered and washed with water and ethanol. Yield: 0.58 g (72%), ^{1}H NMR ($CDCl_3$, 400 MHz): δ ~1.14 (2H, m, CH_2), ~1.39 (8H, m, CH_2), 1.68 (2H, d, CH_2), 1.87 (4H, d, CH_2), 2.03 (4H, d, CH_2) 2.76 (2H, m, CH), 3.92 (8H, s, CH_2), 6.72 (4H, d, PyH), 7.05 (2H, t, PyH). ^{13}C NMR ($CDCl_3$, 400 MHz): δ 159.2, 135.5, 122.5, 67.9, 60.9, 30.2, 26.6. CSI-TOF-MS (in CH_3CN): *m/z* 405.3008 $[M + H]^+$.

Preparation of Precursor Complexes

[Ni(TBDAP)(NO_3)(H_2O)](NO_3). To an acetonitrile solution (2 mL) of $Ni(NO_3)_2{\cdot}6H_2O$ (0.29 g, 1 mmol), a chloroform solution (2 mL) of TBDAP (0.35 g, 1 mmol) was added slowly. The mixture was stirred for overnight. The solvents were removed under vacuum to yield blue powder, which was recrystallized from CH_3CN/Et_2O solution as a blue product. Yield: 0.4 g (75%). Paramagneitc ^{1}H NMR spectrum in SI, Figure S10. UV-vis (CH_3CN): λ_{max} (ε) = 645 nm (10 M^{-1} cm^{-1}), 823 nm (10 M^{-1} cm^{-1}), and 1066 nm (25 M^{-1} cm^{-1}). ESI-MS (CH_3CN): *m/z* 472.2 for $[Ni(TBDAP)(NO_3)]^+$. Anal. Calcd for $C_{22}H_{34}N_6NiO_7$: C, 47.76; H, 6.19; N, 15.19. Found: C, 47.85; H, 5.79; N, 15.33. μ_{eff} = 2.9 BM. X-ray quality crystals were obtained by slow diffusion of Et_2O into a solution of the complex in CH_3CN.

[Ni(CHDAP)(NO_3)](NO_3)(CH_3OH). CHDAP (0.18 g, 0.5 mmol) in chloroform (2 mL) was added to CH_3CN solution (2 mL) of $Ni(NO_3)_2 \cdot 6H_2O$ (0.15 g, 0.5 mmol). The resulting solution was stirred for 12 hours, affording a blue solution. The solvents were removed under vaccum to yield blue powder, which was recrystallized from MeOH/Et_2O solution as a blue crystalline product. Crystalline yield: 0.18 g (75%). Paramagneitc ^1H NMR spectrum in SI, Figure S10. UV-vis (CH_3CN): λ_{max} (ε) = 588 nm (15 M^{-1} cm^{-1}), 835 nm (25 M^{-1} cm^{-1}), and 1010 nm (45 M^{-1} cm^{-1}). ESI-MS (CH_3CN): *m/z* 251.7 for $[Ni(CHDAP)(CH_3CN)]^{2+}$, and 524.3 for $[Ni(CHDAP)(NO_3)]^+$. Anal. Calcd for $C_{27}H_{40}N_6O_7Ni$: C, 52.36; H, 6.51; N, 13.57. Found: C, 52.28; H, 6.30; N, 13.75. μ_{eff} = 3.1 BM.

[Ni(CHDAP)Cl_2]. CHDAP (0.15 g, 0.37 mmol) in dichloromethane (10 mL) was added to suspension of $NiCl_2$ (0.05 g, 0.37 mmol) in CH_3CN (10 mL). The resulting solution was refluxed for 2 days, giving a green solution. The solvents were removed under vacuum to yield solid, which was redissolved in CH_3CN (4 mL). Et_2O and pentane were added to the solution to give a green powder. The green powder was collected by filteration, washed with Et_2O, and dried under vacuum. Yield: 0.17 g (86%). UV-vis (CH_3CN): λ_{max} (ε) = 619 nm (60 M^{-1} cm^{-1}), 659 nm (50 M^{-1} cm^{-1}), and 696 nm (50 M^{-1} cm^{-1}). ESI-MS (CH_3CN): *m/z* 497.2 for $[Ni(CHDAP)Cl]^+$. μ_{eff} = 3.4 BM.

Reference

[1] Koz, G.; Özdemir, N.; Astley, D.; Dincer, M.; Astley. S. T. *J. Mol. Struct.* **2010**, 966, 39-47.

Table S1. Selected bond distances (Å) and angles (º) for [Ni(TBDAP)(NO_3)(H_2O)](NO_3), [Ni(CHDAP)(NO_3)](NO_3)(CH_3OH) and **1**-ClO_4·0.5CH_2Cl_2.

Bond Distances (Å)					
[Ni(TBDAP)(NO_3)(H_2O)](NO_3)		[Ni(CHDAP)(NO_3)](NO_3)(CH_3OH)		**1**-ClO_4·0.5CH_2Cl_2	
Ni1-N1	2.291(2)	Ni1-N1	1.9512(9)	Ni1-N1	1.9195(15)
Ni1-N2	1.977(2)	Ni1-N2	2.1889(9)	Ni1-N2	2.2453(16)
Ni1-N3	2.277(2)	Ni1-N3	1.9429(9)	Ni1-N3	1.9193(15)
Ni1-N4	1.985(2)	Ni1-N4	2.2058(9)	Ni1-N4	2.2901(15)
Ni1-O1	2.0940(17)	Ni1-O1	2.1352(8)	Ni1-O1	1.8589(14)
Ni1-O4	2.0390(18)	Ni1-O2	2.0951(8)	Ni1-O2	1.8670(14)
				O1-O2	1.401(2)
Bond Angles (°)					
[Ni(TBDAP)(NO_3)(H_2O)](NO_3)		[Ni(CHDAP)(NO_3)](NO_3)(CH_3OH)		**1**-ClO_4·0.5CH_2Cl_2	
N1- Ni1-N2	81.30(8)	N1- Ni1-N2	82.32(4)	N1-Ni1-N2	79.85(6)
N1-Ni1-N3	149.30(8)	N1-Ni1-N3	95.64(4)	N1-Ni1-N3	93.82(6)
N1-Ni1-N4	77.45(8)	N1-Ni1-N4	79.40(4)	N1-Ni1-N4	81.99(6)
N2-Ni1-N3	77.73(8)	N2-Ni1-N3	80.42(4)	N2-Ni1-N3	82.96(6)
N2-Ni1-N4	90.51(9)	N2-Ni1-N4	153.22(4)	N2-Ni1-N4	153.17(6)
N3-Ni1-N4	80.55(8)	N3-Ni1-N4	82.08(4)	N3-Ni1-N4	78.71(6)
				O1-Ni1-O2	44.19(7)
				Ni1-O1-O2	68.21(8)
				Ni1-O2-O1	67.60(8)

Table S2. Structural comparison for the nickel(III)-peroxo complexes (Å) in $[Ni(TBDAP)(O_2)]^+$ (**1**) and $[Ni(CHDAP)(O_2)]^+$ (**2**).

	X-ray	DFT	
	$[Ni(TBDAP)(O_2)]^+$	$[Ni(TBDAP)(O_2)]^+$	$[Ni(CHDAP)(O_2)]^+$
avg. Ni-O	1.8630	1.86	1.87
avg. $Ni\text{-}N_{equatorial}$	1.9194	1.93	1.93
avg. $Ni\text{-}N_{axial}$	2.2677	2.30	2.23
O-O	1.401	1.36	1.36

Table S3. Kinetic data for the oxidation of *para*-substituted benzaldehydes by **1** and **2**.

Substrate	**1**	**2**
	k_{obs} (s^{-1})	k_{obs} (s^{-1})
p-tolualdehyde	3.5×10^{-4}	1.4×10^{-3}
4-fluorobenzaldehyde	8.4×10^{-4}	4.1×10^{-3}
Benzaldehyde	1.3×10^{-3}	6.1×10^{-3}
4-chlorobenzaldehyde	2.2×10^{-3}	8.9×10^{-3}
4-bromobenzaldehyde	2.5×10^{-3}	9.9×10^{-3}

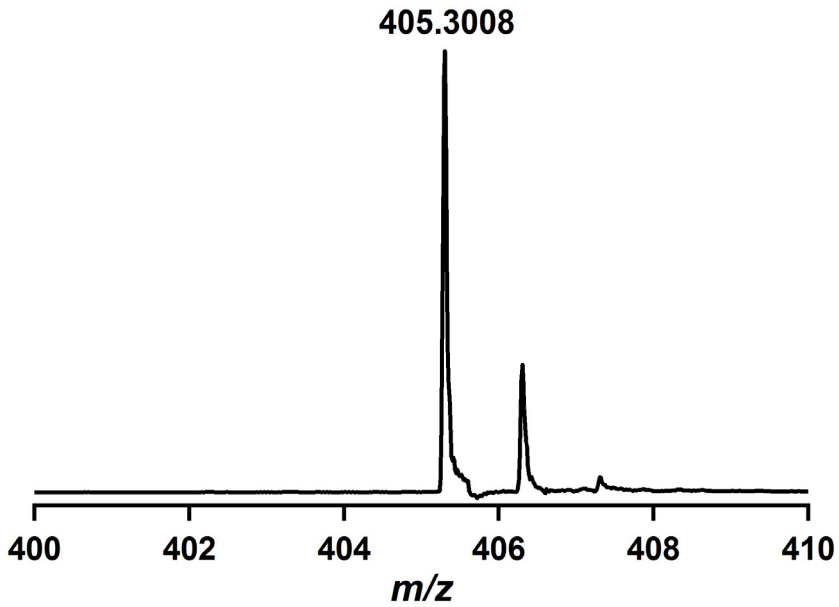

Figure S1. CSI-TOF-MS for the CHDAP ligand in CH_3CN.

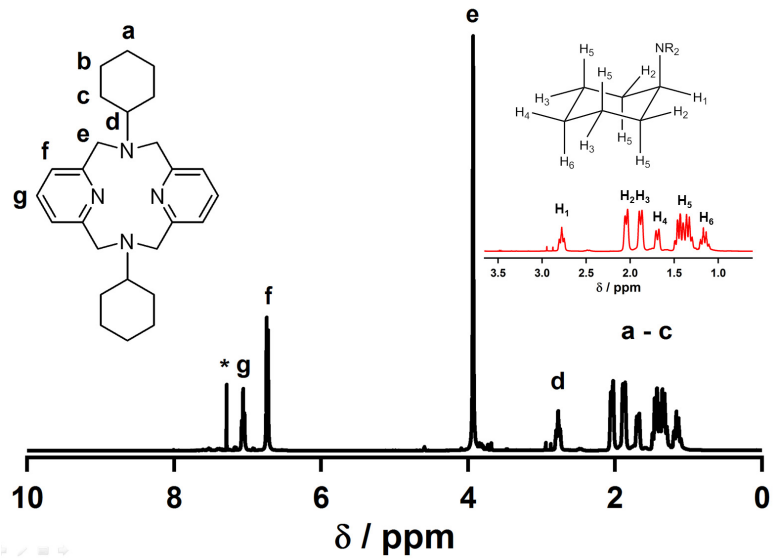

Figure S2. ^{1}H NMR spectrum of the CHDAP ligand in $CDCl_3$ at room temperature. The asterisk is a solvent band. Inset shows the assignments for the signals of the cyclohexyl groups.

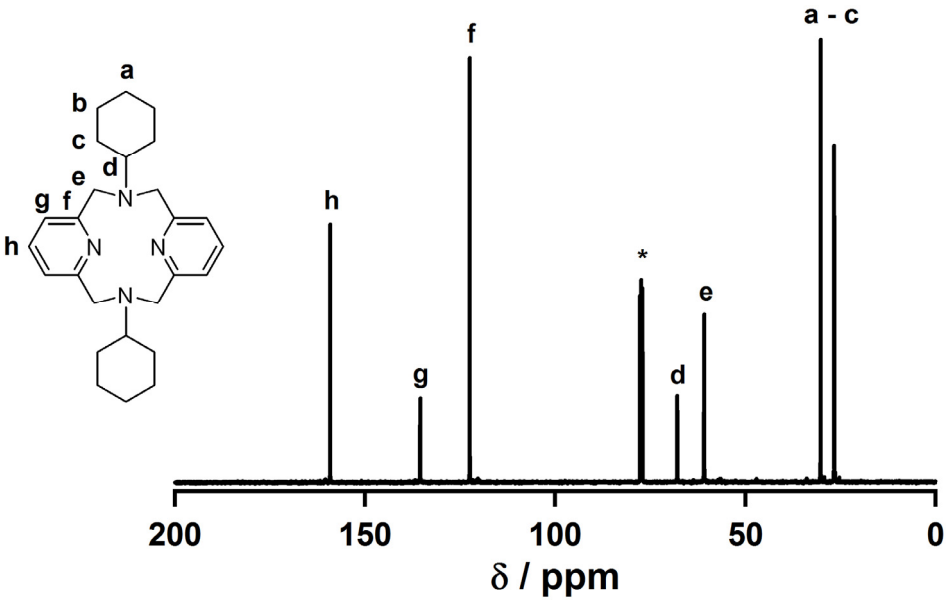

Figure S3. ^{13}C NMR spectrum of the CHDAP ligand in $CDCl_3$ at room temperature. The asterisk is a solvent band.

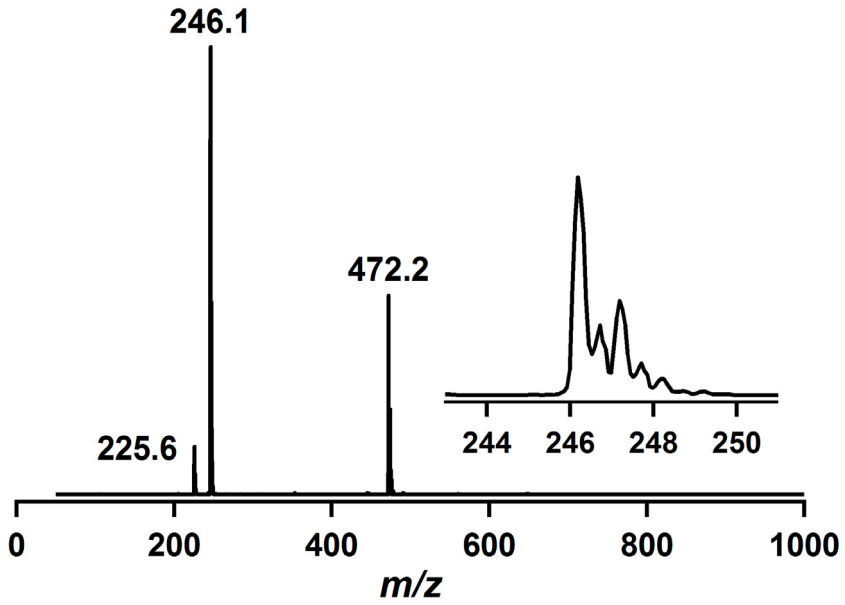

Figure S4. ESI-MS for $[Ni(TBDAP)(NO_3)]^+$ in CH_3CN. Mass peaks at 225.6, 246.1 and 472.2 are assigned to $[Ni(TBDAP)(CH_3CN)]^{2+}$, $[Ni(TBDAP)(CH_3CN)_2]^{2+}$ and $[Ni(TBDAP)(NO_3)]^+$, respectively.

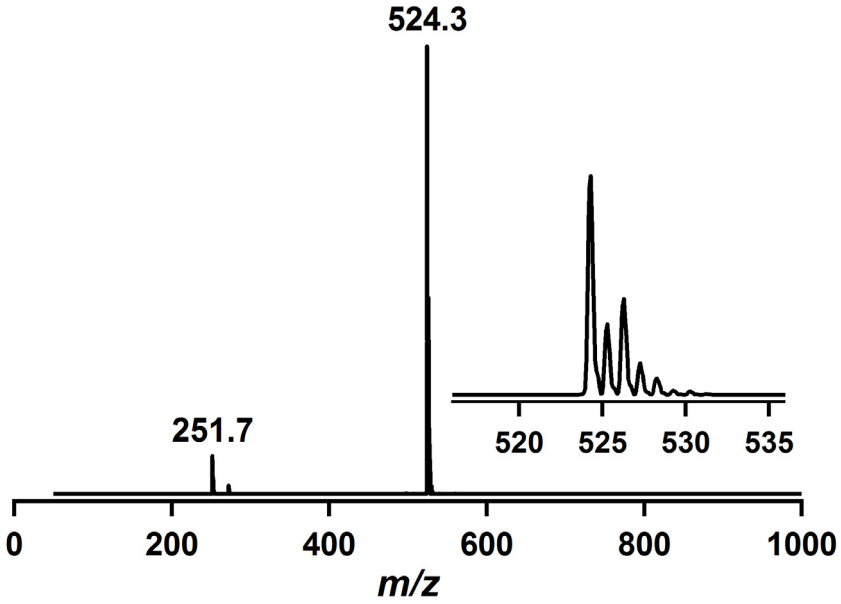

Figure S5. ESI-MS for $[Ni(CHDAP)(NO_3)]^+$ in CH_3CN. Mass peaks at 251.7 and 524.3 are assigned to $[Ni(CHDAP)(CH_3CN)]^{2+}$ and $[Ni(CHDAP)(NO_3)]^+$, respectively.

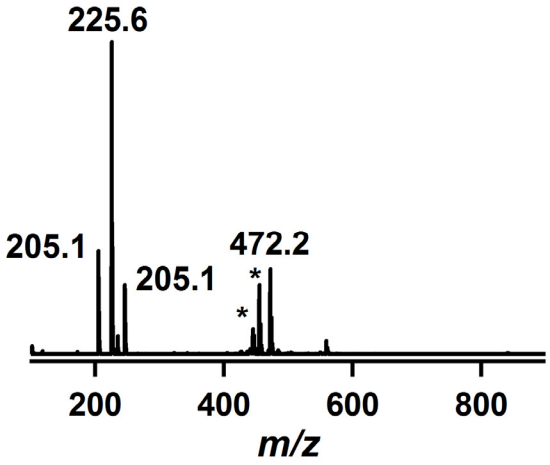

Figure S6. ESI-MS taken after the completion of the reaction of **1** with 2-PPA in CH_3CN at 25 °C, showing the formation of a Ni(II) precursor together with some unidentified species (*): Mass peaks at *m/z* of 205.1, 225.6, 205.1 and 472.2 are assigned to $[Ni(TBDAP)]^{2+}$, $[Ni(TBDAP)(CH_3CN)]^{2+}$, $[Ni(TBDAP)(CH_3CN)_2]^{2+}$ and $[Ni(TBDAP)(NO_3)]^{+}$, respectively.

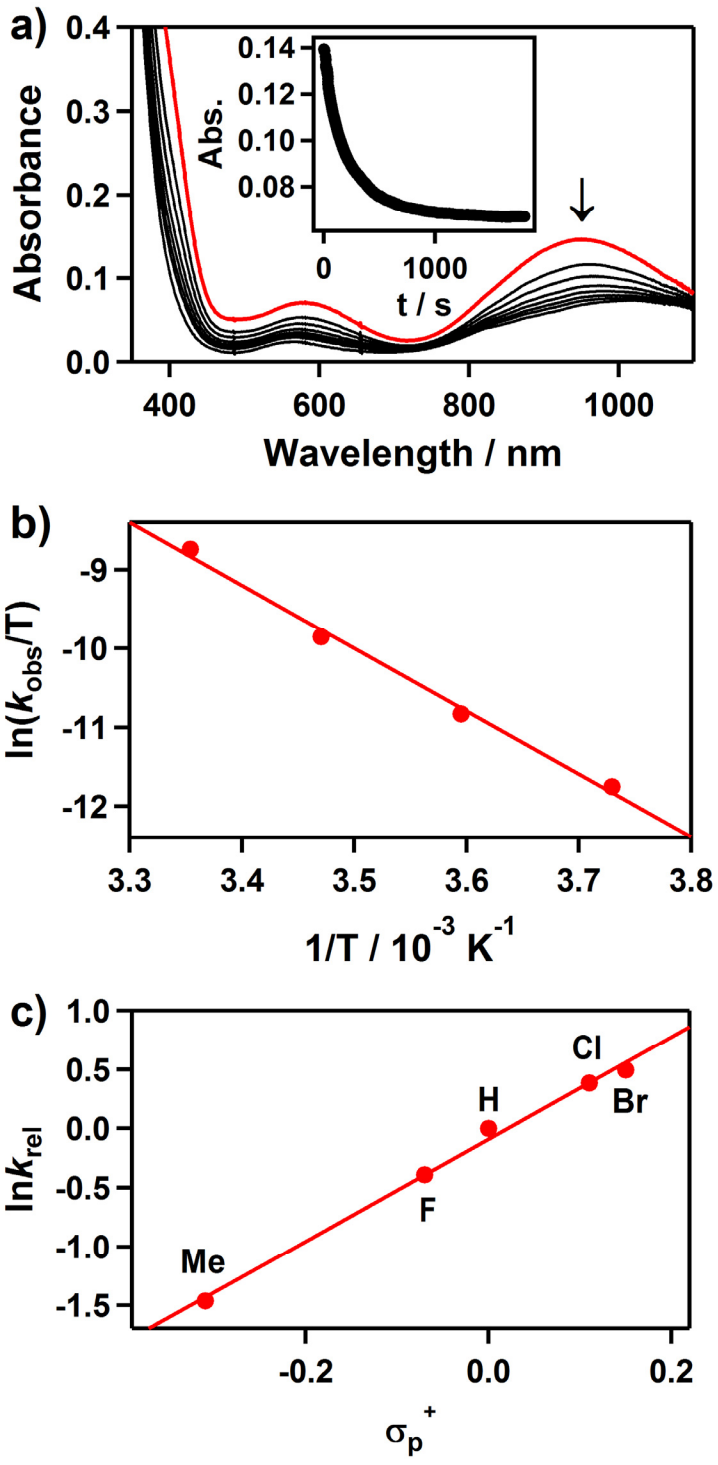

Figure S7. Reactions of $[Ni^{III}(CHDAP)(O_2)]^+$ (**2**) with aldehydes in CH_3CN:CH_3OH (1:1). (a) UV-vis spectral changes of **2** (4 mM) upon addition of 100 equiv. of 2-PPA at 25 °C. Inset shows the time course of the absorbance at 934 nm. (b) Plot of first-order rate constants against $1/T$ to determine activation parameters. (c) Hammett plot of $\ln k_{rel}$ against σ_p^+ of *para*-substituted benzaldehydes. The k_{rel} values were calculated by dividing k_{obs} of *para*-X-Ph-CHO (X = Me, F, H, Cl, Br) by k_{obs} of benzaldehyde at 25 °C.

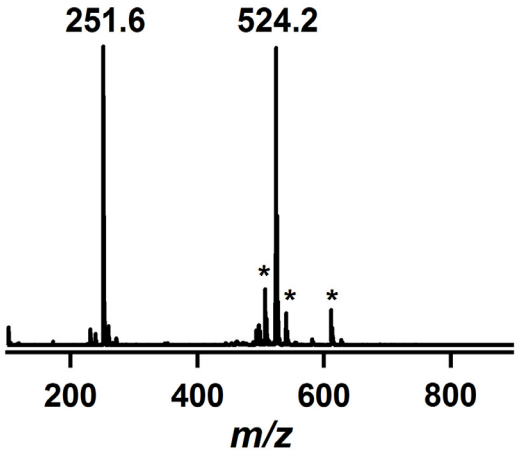

Figure S8. ESI-MS taken after the completion of the reaction of **2** with 2-PPA in CH_3CN at 25 °C, showing the formation of a Ni(II) precursor together with some unidentified species (*): Mass peaks at *m/z* of 251.6 and 524.2 are assigned to $[Ni(CHDAP)(CH_3CN)]^{2+}$ and $[Ni(CHDAP)(NO_3)]^{+}$, respectively.

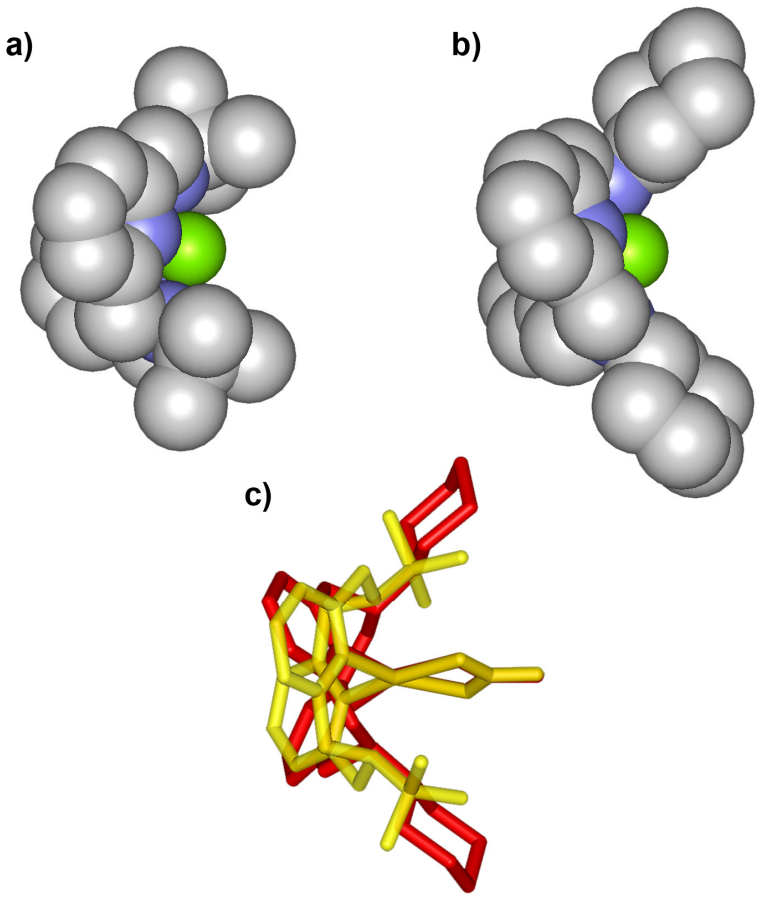

Figure S9. Structural comparison of Ni(II) precursor complexes. Space-filling diagrams of $[Ni(TBDAP)]^{2+}$ (a) and $[Ni(CHDAP)]^{2+}$ (b) moieties taken from the X-ray crystal structures of $[Ni(TBDAP)(NO_3)(H_2O)]^{+}$ and $[Ni(CHDAP)(NO_3)]^{+}$, respectively, where NO_3^- and H_2O molecules are omitted for clarity (C, gray; N, blue; Ni, green). (c) Overlay of the molecular structures of Ni(II) precursors with TBDAP (yellow) and CHDAP (red), illustrating difference in the steric effect on *tert*-butyl vs cyclohexyl groups toward the nickel center. Although the structure of $[Ni(TBDAP)(NO_3)]^{+}$ is plagued by problems of low-quality crystals, the data were sufficient to show the difference of substituents.

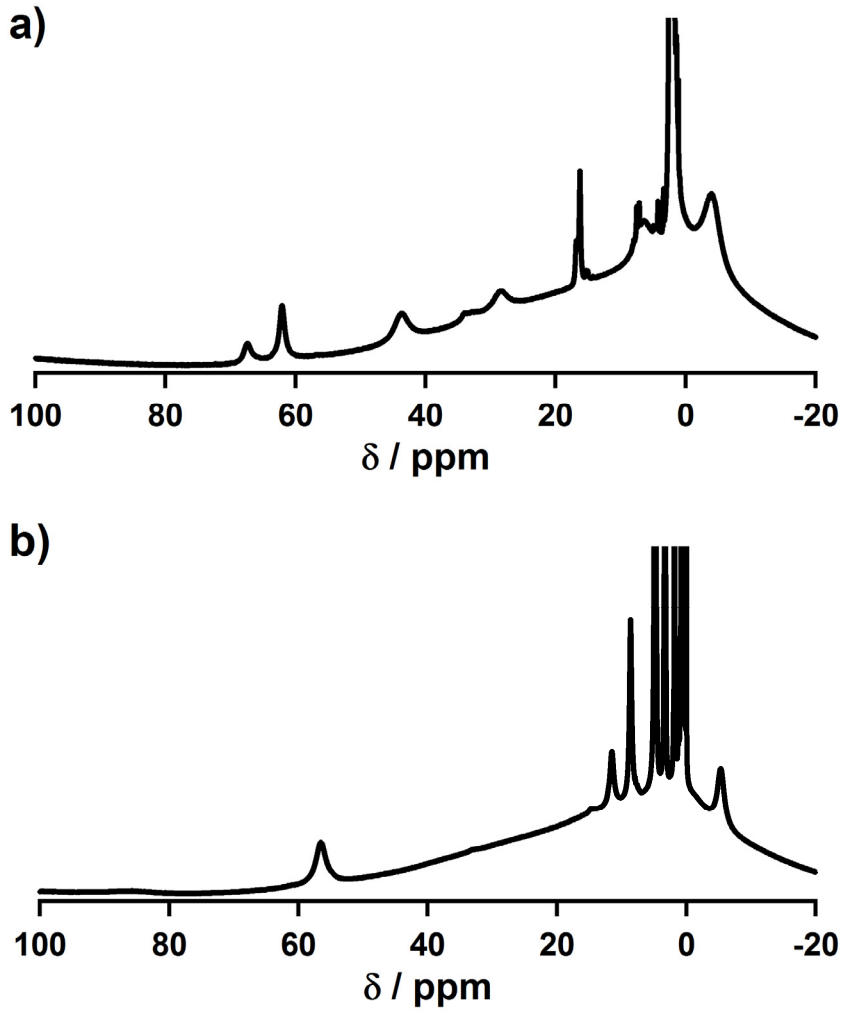

Figure S10. The Paramagnetic ^{1}H NMR spectra of (a) $[Ni(TBDAP)(NO_3)(H_2O)]^+$ and (b) $[Ni(CHDAP)(NO_3)]^+$ in CD_3CN at room temperature.